

INTERAGENCY AGREEMENT BETWEEN NATIONAL PARK SERVICE
and
NASA/Goddard Space Flight Center
Cryospheric Sciences Branch, Code 614.1

Project Title:

Change Analysis of Glacier Ice Extent and Coverage for three Southwest Alaska
Network (SWAN) Parks – Katmai National Park and Preserve, Kenai Fjords
National Park, and Lake Clark National Park and Preserve

Dorothy K. Hall
NASA/GSFC
(Dorothy.k.Hall@nasa.gov)

Bruce A. Giffen
NPS
(Bruce_Giffen@nps.gov)

and

Janet Y.L. Chien
SAIC, Inc. and NASA/GSFC
(Janet@glacier.gsfc.nasa.gov)

April 19, 2005

Changes in the Harding Icefield and the Grewingk-Yalik Glacier Complex, Kenai
Fjords National Park (KEFJ)

Abstract

Glacier changes in the mountains of the Kenai Peninsula, Alaska, have been analyzed in the Harding Icefield and the Grewingk-Yalik Glacier Complex in Kenai Fjords National Park (KEFJ). Glaciers that originate in the park, and flow outside of the park are also included. The Harding Icefield spawns more than 38 glaciers of which some are tidewater and others are land-based, or wholly or partially terminate in lakes. We used Landsat Multispectral Scanner (MSS), Thematic Mapper (TM) and Enhanced Thematic Mapper Plus (ETM+) scenes to outline glacier areas and terminus positions on four scenes. Glacier outlines were done using vector segments to produce shape files for the Geographic Information System (GIS) analysis. Results show that most of the glaciers in KEFJ have receded since 1973, some dramatically. These results are generally consistent with results from extensive work done in the 1990s on the Harding Icefield by previous researchers. For this project, we derived GIS shape files,

and from those we can calculate glacier area and terminus changes from 1973 to 2002, and estimate the 1986 equilibrium-line altitude (ELA) for the large glaciers. We also did a classification of the 1986 and 2002 Landsat scenes to measure the areal extent of the two ice masses, and found that there was a reduction of 3.62%, or approximately 78 km² from 1986 to 2002, with most of the changes occurring in the Harding Icefield. Some issues that complicate the analysis include: fresh snow cover and spatial resolution differences between images.

Introduction

Glacier changes have been analyzed in the Harding Icefield and the Grewingk-Yalik Glacier Complex of Kenai Fjords National Park (KEFJ). Glaciers that originate in the park, and flow outside of the park are also included. We used Landsat Multispectral Scanner (MSS), Thematic Mapper (TM) and Enhanced Thematic Mapper Plus (ETM+) scenes to determine glacier areas and positions of the glacier termini. Three years of Landsat scenes were used: 1973, 1986 and 2002. We also used a digital-elevation model (DEM) that was derived from a 29 September 2001 Landsat scene.

Outlines of all of the glaciers were traced using vector segments to produce Geographic Information System (GIS) shape files on each Landsat image in 1973, 1986 and 2002, and the terminus-position change on many glaciers was measured.

Results are consistent with previous work on the Harding Icefield and provide updated quantitative information on glacier area and terminus change on all of the major glaciers (both inside and outside of KEFJ) in the Harding Icefield and the Grewingk-Yalik Glacier Complex which is located to the south of the Harding Icefield. GIS shape files can be used in future analyses to measure changes to compare with the 1973, 1986 and 2002 areal extent and terminus positions of the glaciers provided.

Background

The Earth's small glaciers are sensitive indicators of regional and global climate, especially since small glaciers are found on all continents except Australia. Globally, small glaciers have generally been receding on all continents (Dyurgerov and Meier, 1997), with the exception of Antarctica where the mass balance of the ice sheet is poorly known. As the Earth's climate warms, such as is occurring at present, meltwater from small glaciers contributes to sea-level rise (SLR).

The Earth's glaciers have been studied in a coordinated way in the last 50 years or so. A notable example is the work of Bill Field resulting in the publication of

his two-volume book set and atlas of mountain glaciers of the Northern Hemisphere (Field, 1975). More recently, the *Satellite Image Atlas of the World*, a multi-decade project that will culminate in 2006, is a series of 11 volumes written by an international team of 80 scientists from 25 nations. It uses Landsat images from 1972 to the present to establish a baseline of the area covered by the Earth's glaciers (for example, see Williams and Ferrigno, 1993). The remaining volumes are now being completed and published in print and digital formats [[http://pubs.usgs.gov/prof/p1386\(a-k\)](http://pubs.usgs.gov/prof/p1386(a-k))]. The Advanced Spaceborne Thermal Emission and Reflection Radiometer (ASTER)-based Global Land Ice Imaging from Space (GLIMS) Project is well underway, thus providing an excellent follow-on to the Glacier Atlas series (Kieffer et al., 2000), and to earlier efforts to map glaciers globally. The overarching objective of the GLIMS project is to measure quantitatively changes in the areal extent of the Earth's glaciers and to maintain a database of GIS shape files of glacier area globally. The international GLIMS team uses high-resolution satellite images from the EOS satellites (ASTER and Landsat) to monitor the changing size and terminus fluctuations of glaciers.

Alaska glaciers are significant contributors to SLR, contributing ~9% of the observed rate of SLR (1.5 ± 0.5 mm/yr) over the last 50 years (Arendt et al., 2002). Harding Icefield, named for former U.S. President Warren Harding, is located in the mountains of the Kenai Peninsula, Alaska. The icefield spawns more than 38 glaciers some of which are tidewater, some of which terminate in lakes, and others terminate on land. Harding Icefield is ~80 km long and 50 km wide, covering an area of ~1800 km². About half of the icefield lies within the present boundary of KEFJ. The Harding Icefield has been thinning and shrinking since the 1950s (Adalgeirsdóttir et al., 1998).

The Harding Icefield was the focus of extensive work during the 1990s (Echelmeyer et al., 1996; Adalgeirsdóttir et al., 1998; Sapiano et al., 1998). Echelmeyer et al. (1996) used an airborne altimetry system consisting of a nadir-pointing laser rangefinder mounted in a small aircraft and a gyro to measure the orientation of the ranger, and GPS methods for continuous measurement of aircraft position. Profiles were flown along centerlines of main glacier trunks and major tributaries at elevations of 50 – 300 m above the ground, and compared with contours on 15-min USGS topographic maps made from aerial photographs acquired from the 1950s to the 1970s. They used the altimetry data to calculate differences in elevation at profile/contour line intersection points.

Specifically, Adalgeirsdóttir et al. (1998) obtained airborne surface-elevation profiles in 1994 and 1996 of a total of 13 glaciers in the Harding Icefield and compared the elevations with USGS topographic maps from the 1950s to determine elevation and volume changes. They estimated that the total volume change for this ~43-year period was -34 km³, which corresponds to an area-average elevation change of -21 ± 5 m. Many glaciers below ~1000 m disappeared.

Procedures for analysis of KEFJ glaciers

Four Landsat scenes, shown in **Table 1**, were used in the analysis. These scenes are georeferenced. Note that measurements that were made in 2002 were made on the 9 August scene except when clouds precluded measurement; in those cases, the 30 July scene was used.

Table 1. Landsat scenes used in the study.

Date	Sensor	Scene i.d. number
17 August 1973	MSS	LM1074018007322990
12 September 1986	TM	LT5069018008625510
30 July 2002*	ETM+	LE7069018000221150
09 August 2002	ETM+	LE7069018000022250

*Only used when key parts of the 9 August 2002 scene were cloudy

The 12 September 1986 Landsat scene is the best quality of the Landsat scenes in terms of minimizing cloud cover and snow cover. This image serves as the reference image for the project. The KEFJ boundary, a shape file, was digitally added on the image. A grid was placed over the park to make it easy to locate specific glaciers during the subsequent analysis (**Figure 1**). Using PCI image-processing software, the outlines of most of the glaciers in the park were traced on each Landsat image. Very small glaciers, and areas that appeared to be snowfields (not glacier ice) were generally not traced. Most glaciers that emanate in the park, but terminate outside of the park were also traced.

Following near-finalization of the preliminary outlines, the entire outlining process was repeated using vector segments to produce GIS shape files. Glacier termini are usually not straight across and they do not necessarily move back (or forward) in a straight line and therefore the point that can be selected to measure the glacier is highly variable. When we measured terminus-position change, we selected points that represent the greatest change. Thus we use the word “approximate” when referring to glacier recession. If we had selected different points, the amount of glacier recession would have been different.

The georeferenced images were also used to measure the approximate location of the ELA on the largest glaciers in the park from the location of the seasonal snowline on the 1986 image. While it is not possible to measure the ELA reliably from space, often the snowline or the firn limit is easily mapped from space and can sometimes approximate the location of the ELA (see [Williams et al., 1991](#)). Of the three years studied, only the image from 12 September 1986 was suitable

for analysis of the elevation of the firn line because snow cover on the other three images precluded determination of the elevation of the snowline.

Much work has been done to derive the ELA from synthetic aperture radar (SAR) images (see for example, [Fahnestock et al., 1993](#)), however, many issues remain before this method can be considered to be reliable as discussed in [Hall et al. \(2000\)](#).

Determination of measurement errors

The Landsat MSS, launched in 1972, provided images with a pixel resolution of 80 m. Not until the launch of the Landsat-4 satellite in 1982 did the resolution of the imagery improve with the TM sensor (pixel resolution of 30 m). The amount of detail possible to discern using MSS imagery is less as compared to when TM data are used, and the errors are greater when comparing glacier changes from MSS to TM scenes, than when comparing changes seen on TM scenes or between TM and ETM+ scenes. When measuring the change in a glacier terminus position from the 1973 MSS image, to a TM or ETM+ image, the error is ± 136 m. When measuring changes from 1986 to 2002, using TM and ETM+ images, the error is ± 54 m. See [Hall et al. \(2003\)](#) for a discussion of measurement errors with respect to glacier area and terminus measurements from Landsat data. Because all of the Landsat scenes are georeferenced, there are no image-registration errors in connection with the present analysis.

Results of the analysis of terminus changes

Most of the glaciers in KEFJ have receded since 1973; some have moved back dramatically. Some glaciers, however, have shown very little change, and a few have moved forward.

The tidewater glaciers flowing to the east in KEFJ terminate in the Gulf of Alaska; tidewater glaciers are known to have a cycle that is not necessarily directly related to short-term climate change ([Meier and Post, 1987](#)). Glaciers that presently terminate in tidewater in KEFJ include the Aialik, Bear, Holgate, McCarty and Northwestern.

In general, land-based glaciers are known to be generally responsive to short-term climate change (however there are many exceptions to this). Examples of land-based glaciers inside and just outside of the park include the Chernof, Exit, Indian, Katchemak, Killey, Lowell, Nuka, Pedersen, Petrov, Skilak, Tustumena and Yalik, some of which terminate wholly or partly in a lake (see **Table 2**).

All of the glaciers (with the exception of very small glaciers or snow fields as noted above) in KEFJ were outlined on 1973, 1986 and 2002 Landsat scenes, as

were many glaciers that terminate outside of KEFJ. Changes in the terminus positions and approximate rates of recession (in m a^{-1}) are given in **Table 2**. Most of the glaciers are not shown in **Table 2** because of the difficulty in getting a meaningful terminus-change measurement, but their outlines are provided as shape files. Furthermore, the numbers that are shown in **Table 2** are approximate because they are highly dependent on the exact spot on the terminus that we selected to make the measurement.

Table 2. Change (in m) of the terminus position* of selected glaciers in Kenai Fjords National park; average annual rate of change (in m a^{-1}) is shown in parentheses. A negative sign (-) means that the glacier receded. Errors were determined from [Hall et al. \(2003\)](#).

*The terminus "position" can be measured at various points along the edge of the glacier in each year. For each glacier, we have chosen the part of the terminus that shows the greatest change. Because of the irregularity of the terminus, and the arbitrary nature of selecting a point from which to measure, these measurements may not be repeatable.

Glacier name	Change (in m) from 1973-1986; average annual rate of change (in m a^{-1}) is shown in parentheses	Change (in m) from 1986-2002; average annual rate of change (in m a^{-1}) is shown in parentheses	Change (in m) from the 1950s to the 1990s (from Adalgeirsdóttir et al. (1998) , Table 6)
Aialik ¹	-85±136 (-7)	-95±54 (-6)	+540
Bear ^{2,3}	extensive recession, but difficult to measure	extensive recession, but difficult to measure	⁴ -1550
Chernof ³	-162±136 (-13)	-339±54 (-21)	⁵
Dinglestadt ²	-566±136 (-44)	-474±54 (-30)	⁵
Exit (south edge of terminus) ³	-134±136 (-10)	+95±54 (+16)	-490
Holgate ¹	-319±136 (-25)	no change	-260
Indian ³	-234±136 (-18)	-180±54 (-11)	⁵
Katchemak ³	-283±136 (-22)	-67±54 (-4)	-900
Killey ³	-268±136 (-21)	-446±54 (-28)	⁵
Lowell ³	-272±136 (-21)	-708±54 (-44)	⁵
Northwestern ¹	-67±136 (-5)	-2184±54 (-137)	-4200
McCarty ¹	+583±136 (+45)	-306±54 (-19)	-690
Nuka ³	-302±136 (-23)	no change	⁵
Pedersen ^{2,3}	-511±136 (-39)	-108±54 (-7)	⁵
Petrof ³	-730±136 (-56)	-371±54 (-23)	⁵
Skilak ²	-2290±136 (-176)	-1521±54 (-95)	-3200
Tustumena northern ²	-1856±136 (-143)	+537±54 (+34)	⁵
Yalik ²	-726±136 (-56)	-579±54 (-36)	⁵

¹Terminates in tidewater

²Terminates in a lake

³Terminates on land

⁴ Sapiano et al. reported a recession of -515 m of the Bear Glacier terminus, and a decrease in average thickness (-12.5 ± 2.8 m) from 1957-1996, thus not in agreement with the change reported by [Adalgeirsdóttir et al. \(1998\)](#).

⁵ Not reported

The Skilak Glacier (**Figure 2**) has shown dramatic recession, especially from 1973-1986. The Lowell (**Figure 3**), Petrof (**Figure 4**) and Pedersen Glaciers have receded steadily since 1973. The terminus of the Northwestern Glacier, a tidewater glacier, did not change much from 1973 to 1986, but moved back quite dramatically between 1986 and 2002. The terminus of the unnamed glacier that is located southeast of the Northwestern Glacier and flowing toward Striation Island in Northwestern Lagoon, is currently land based, and is shown in **Figure 5** to have receded and broken up dramatically from 1973 to 2002.

The McCarty Glacier (**Figure 6**) is a tidewater glacier that advanced from 1973 to 1986, and then retreated from 1986 to 2002.

Preliminary analysis indicates that the glaciers in KEFJ have generally receded, and probably the recession of the land-based glaciers is due to a regional warming of the summer temperatures as has been discussed by [Arendt et al. \(2002\)](#) following their extensive analyses of glaciers in southern Alaska. Some meteorological data are now available but have not yet been analyzed for the present work.

Areal extent of Harding Icefield

The areal extent of both the Harding Icefield and the Grewingk-Yalik Glacier Complex was also measured using a supervised-classification technique. Because of the resolution difference between the MSS and TM or ETM+ data, it is difficult to make a meaningful comparison of the 1973 with the 1986 or 2002 measurements shown in **Table 3**, so the 1973 measurement is not shown. However, it is reasonable to compare the 1986 and 2002 measurements although it is not possible to ascribe an accuracy to these measurements. A reduction of about 3.62% (78 km²) was measured between 1986 and 2002 and is depicted in **Figure 7** as a difference map, with most of the change occurring in the Harding Icefield, and very little change was measured in the Grewingk-Yalik Glacier Complex. It was difficult to determine exactly what ice masses to use in the comparison because some small glaciers may or may not be part of the Harding Icefield. However, the same ice masses were measured in both years, so the relative change in areal extent between years was captured in the measurements.

Table 3. Extent of the Harding Icefield and the Grewingk-Yalik Glacier Complex as measured using Landsat data (in km²).

Year	Total Area (km ²)	Harding Icefield (km ²)*	Grewingk-Yalik Glacier Complex (km ²)
1986	2156	1753	403
2002	2078	1679	399

*Adalgeirsdóttir et al. (1998) state that the extent of the Harding Icefield is ~1800 km².

During the supervised classification, there were numerous, but isolated pixels that were obviously not ice, but were classified as ice on both scenes, so these pixels were deleted, manually, from the analysis. These pixels were not connected to the main bodies of ice. They may represent isolated snow patches, or, more likely, other features that have a spectral reflectance similar to snow and ice. Other glaciers that were not connected to the Harding Icefield were also not considered in the measurements shown in **Table 3** because it was not clear whether or not they are actually considered to be part of the Harding Icefield.

Complicating issues

Some issues that complicate the analysis include: fresh snow cover, resolution differences between images and difficulty in determining the equilibrium line. If the timing of a new snowfall is such that it obscures the location of the snowline or firn limit on a Landsat image of a glacier even if the new snow melts after a few hours or a day, then the firn limit may not be possible to measure using Landsat data. The other complication with fresh snow is that, at the lower elevations, it can cause very small glaciers or permanent snow fields to appear larger than they really are thus making their true extent impossible to measure, accurately, using Landsat data.

Another issue is the difficulty in determining the exact change of a glacier terminus when it is covered with debris. Additionally, using Landsat data, icebergs may sometimes be difficult to distinguish from glacier ice in the case of glaciers that terminate in tidewater or a lake as in the case of the Skilak Glacier as seen in **Figure 2**.

Discussion and Conclusions

All land-based glaciers for which the terminus position was measured and shown in **Table 2** in KEFJ receded from 1973 to 2002, with the exception of the Nuka Glacier (no change measured from 1986-2002) and the northern arm of the

Tustumena Glacier (537 m advance from 1986-2002). Of the four tidewater glaciers listed in **Table 2**, two (Aialik and Northwestern) retreated, but the McCarty experienced a net advance between 1973 to 2002, and the Holgate advanced from 1973-1986, but then did not change from 1986-2002. It is very difficult to compare our terminus-change measurements with those measurements by [Adalgeirsdóttir et al. \(1998\)](#) based on measurements made in the 1990s because all of the measurements depend upon the exact location selected on the terminus, though the trends generally agree.

Measurement of the areal extent of the Harding Icefield and the Grewingk-Yalik Glacier Complex using a supervised-classification technique, in 1973, 1986 and 2002, shows a reduction in extent of the icefields from 1986 to 2002, of 3.62% or about 78 km², however the measurement errors are difficult to determine and may be large. The 1973 measurement is not shown due to the extreme difficulty in performing a meaningful classification of the areal extent of the icefield using the 80-m resolution MSS imagery.

Possible future work

Additional work could be done in the Harding Icefield in order to perform a more thorough analysis of the glaciers in KEFJ. Shape files could be created using 15-m resolution ASTER or ETM+ (band 8) imagery. ASTER scenes were acquired free of charge (by DKH). The addition of the ASTER imagery may provide more detailed information on a few glaciers that were imaged by the ASTER, though only a few cloud-free ASTER scenes are available that are of sufficiently good quality to perform the analysis. All glaciers could be analyzed in more detail using band 8 (panchromatic band) of the ETM+ from two 2002 scenes. The advantage of the more-detailed analysis would be that shape files from future high-resolution sensors could be compared with these data providing finer detail than is possible with the 30-m resolution data.

Air photos, obtained by the National Park Service in 1993 and 1994, could also be studied in detail, and shape files could be provided for some of the glacier areas using the air photos as well. For some glaciers, the terminus positions from the air photos could be compared with the terminus positions as determined from Landsat data. This would improve our ability to assign errors to the Landsat work, and may help to resolve some issues related to debris-covered termini.

The glacier-facies concept was developed by Carl Benson ([Benson, 1962 & 1996](#)) following a series of field observations on the western margin of the Greenland Ice Sheet in the 1950s. A glacier may be divided into an accumulation and an ablation area, and the line that divides those parts of a glacier is termed the equilibrium line. The equilibrium-line altitude (ELA) is the elevation at which this divide occurs. For many valley and outlet glaciers in temperate climates, the position of the snowline at the end of an average mass-

balance year represents the approximate location of the equilibrium line, and the firn limit can often be discerned from satellite data if the image was acquired at the end of the melt season (Williams et al., 1991).

The approximate elevation of the ELA on some of the largest glaciers in KEFJ was determined for 1986 as a baseline for future work. However elevations are not given because the exact elevation of the ELA is dependent upon where on the glacier it is measured. In the future, the shape files for the largest glaciers in the park need to be provided as determined from the 1986 scene. This is the only scene of the three in which the snow cover extent is small enough to allow measurement of an approximate maximum height of the firn line.

Furthermore, analysis of the meteorological data from Seward should also be studied in the context of changes in the KEFJ glaciers.

References

Adalgeirsdóttir, G., K.A. Echelmeyer and W.D. Harrison, 1998: Elevation and volume changes on the Harding Icefield, Alaska, *Journal of Glaciology*, 44(148):570-582.

Arendt, A.A., Echelmeyer, K.A., Harrison, C.A., Lingle, C.A. and Valentine, V.B. 2002: Rapid wastage of Alaska glaciers and their contribution to rising sea level. *Science*, 297:382-386.

Benson, C.S. (1962 & 1996): Stratigraphic studies in the snow and firn of the Greenland ice sheet, Snow, Ice and Permafrost Research Establishment (now U.S. Army Cold Regions Research and Engineering Laboratory), Research Report 70 (reprinted and updated in 1996), 93 p. + appendices.

Dyrgerov, M. and M. Meier, 1997: Mass balance of mountain and subpolar glaciers: a new global assessment for 1961-1990, *Arctic and Alpine Research*, 27(4):379-391.

Echelmeyer, K.A., W.D. Harrison, C.F. Larsen, J. Sapiano, J.E. Mitchell, J. DeMallie, B. Rabus, G. Adalgeirsdóttir, and L. Sombardier, 1996: Airborne surface profiling of glaciers: a case-study in Alaska, *Journal of Glaciology*, 42(142):538-547.

Fahnestock, M., R. Bindshadler, R. Kwok and K. Jezek, 1993: Greenland ice sheet surface properties and ice dynamics from ERS-1 SAR imagery, *Science*, 262(5139):1530-1534.

Field, W.O. (ed.), 1975: *Mountain Glaciers of the Northern Hemisphere*, vols. 1&2, Cold Regions Research and Engineering Laboratory, Hanover, NH.

Hall, D.K., R.S. Williams, Jr., J.S. Barton, O. Sigurdsson, L.C. Smith and J.B. Garvin, 2000: Evaluation of remote-sensing techniques to measure decadal-scale changes of Hofsjökull ice cap, Iceland, *Journal of Glaciology*, 46(154):375-388).

Hall, D.K., K.J. Bayr, W. Schöner, R.A. Bindschadler, J.Y.L. Chien, 2003: Changes in the Pasterze and the Kleines Fleißkees glaciers, Austria, as Measured from the Ground and Space, *Remote Sensing of Environment*, 86:566-577.

Kieffer, H. et al., 2000: New Eyes in the Sky Measure Glaciers and Ice Sheets, *Eos, Transactions, American Geophysical Union*, 2000-06-13, 81:265, 270-271.

Meier, M. and A. Post, 1987: Fast tidewater glaciers, *Journal of Geophysical Research*, 92:9051-9058.

NPS, 2002: Kenai Fjords National Park map, National Park Service.

Sapiano, J.J., W.D. Harrison and K.A. Echelmeyer, 1998: Elevation, volume and terminus changes of nine glaciers in North America, *Journal of Glaciology*, 44(146):119-135.

Williams, R.S., Jr., D.K. Hall, and C.S. Benson, 1991: Analysis of Glacier Facies Using Satellite Techniques, *Journal of Glaciology*, 37:120-128.

Williams, R.S., Jr. and Ferrigno, J.G., 1993: Satellite image atlas of glaciers of the world - Europe, U.S. Geological Survey Professional Paper 1386-E, 164 p.

Figures

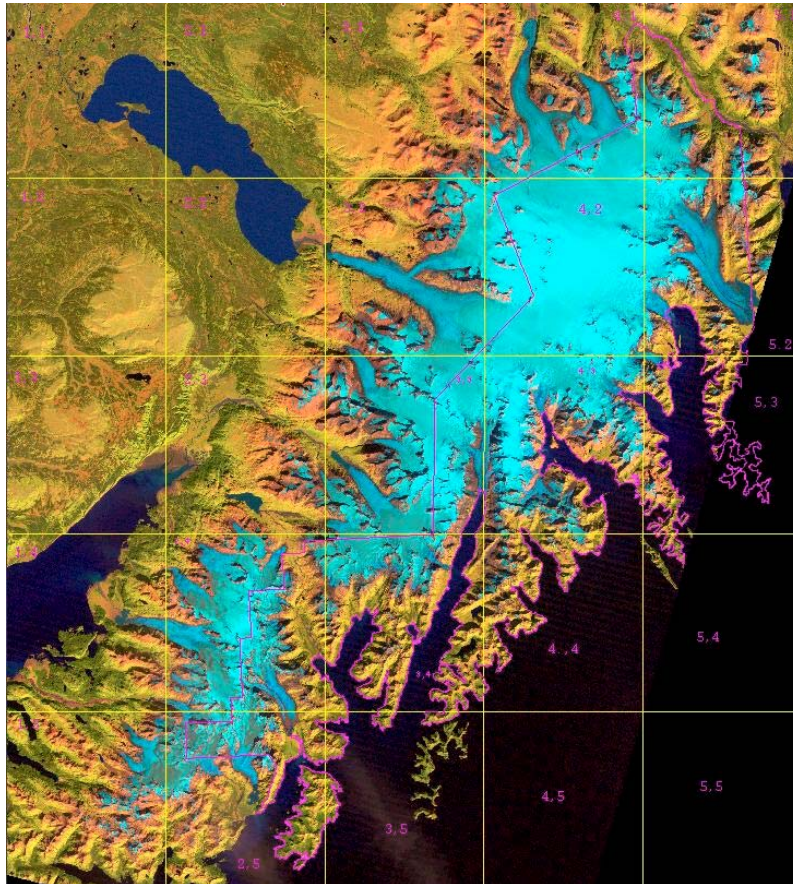


Figure 1. 12 September 1986 Landsat Thematic Mapper image showing an overview of the Harding Ice Field. The grid shows the manner in which the area was divided for the analysis. The Kenai Fjords National Park outline is shown in purple.

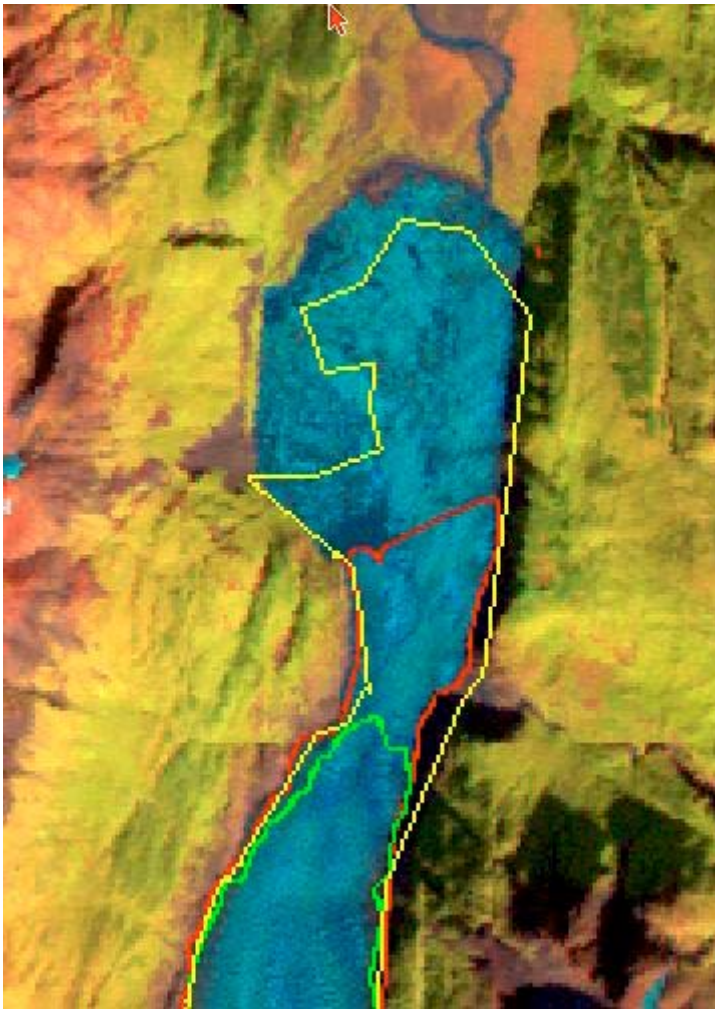


Figure 2. 12 September 1986 Landsat Thematic Mapper TM image showing the terminus of the Skilak Glacier. The yellow line represents the position of the glacier terminus as measured from the 17 August 1973 image, the red line represents the position in 1986, and the green line represents the terminus position as measured from the 9 August 2002 ETM+ image (or the 30 July 2002 ETM+ image if clouds obscured the area on the 9 August 2002 image).

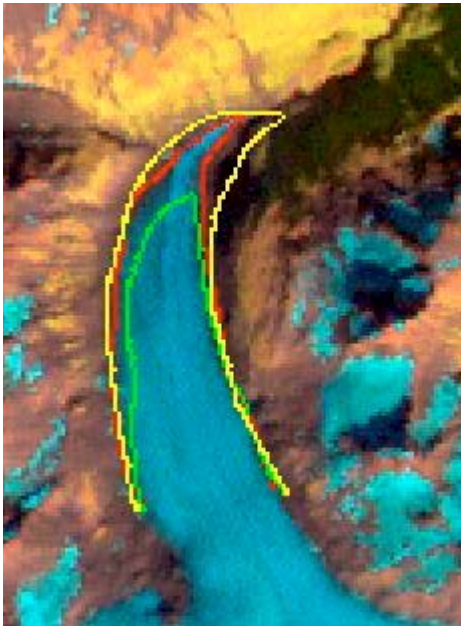


Figure 3. 12 September 1986 Landsat Thematic Mapper TM image showing the terminus of the Lowell Glacier. The yellow line represents the position of the glacier terminus as measured from the 17 August 1973 image, the red line represents the position in 1986, and the green line represents the terminus position as measured from the 9 August 2002 ETM+ image (or the 30 July 2002 ETM+ image if clouds obscured the area on the 9 August 2002 image).

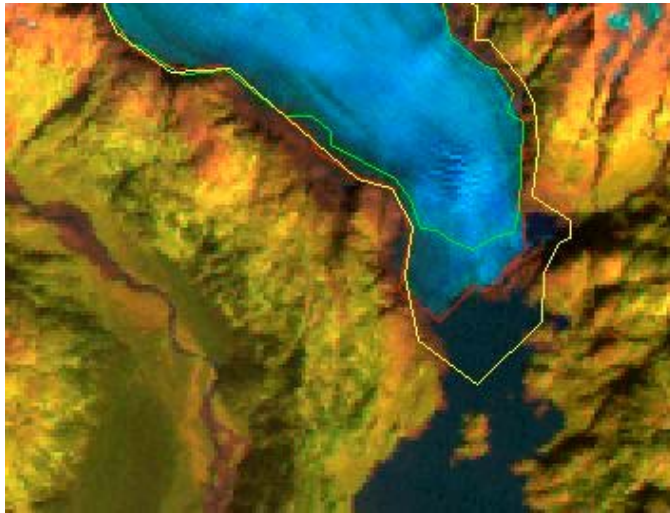


Figure 4. 12 September 1986 Landsat Thematic Mapper TM image showing the terminus of the Petrof Glacier. The yellow line represents the position of the glacier terminus as measured from the 17 August 1973 image, the red line represents the position in 1986, and the green line represents the terminus position as measured from the 9 August 2002 ETM+ image (or the 30 July 2002 ETM+ image if clouds obscured the area on the 9 August 2002 image).

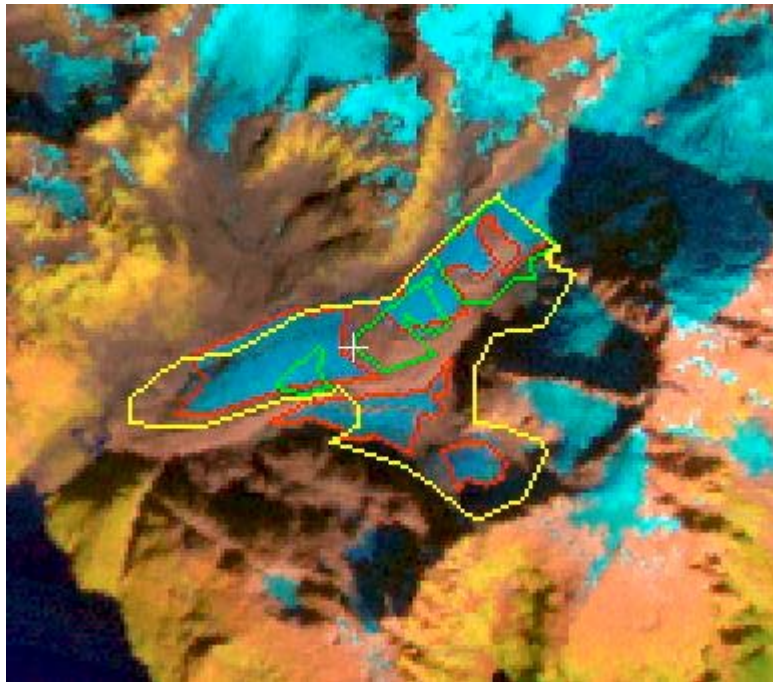


Figure 5. 12 September 1986 Landsat Thematic Mapper TM image showing the terminus of the unnamed glacier located to the southeast of the Northwestern Glacier and flowing toward Striation Island in Northwestern Lagoon. The yellow line represents the position of the glacier terminus as measured from the 17 August 1973 image, the red line represents the position in 1986, and the green line represents the terminus position as measured from the 9 August 2002 ETM+ image (or the 30 July 2002 ETM+ image if clouds obscured the area on the 9 August 2002 image).

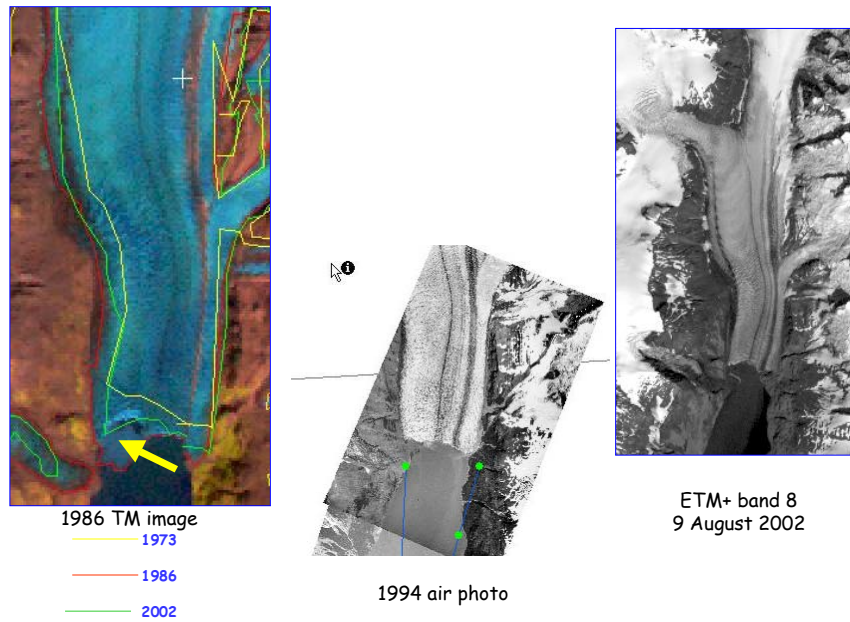


Figure 6. Landsat images and an air photo of the terminus of the McCarty Glacier.

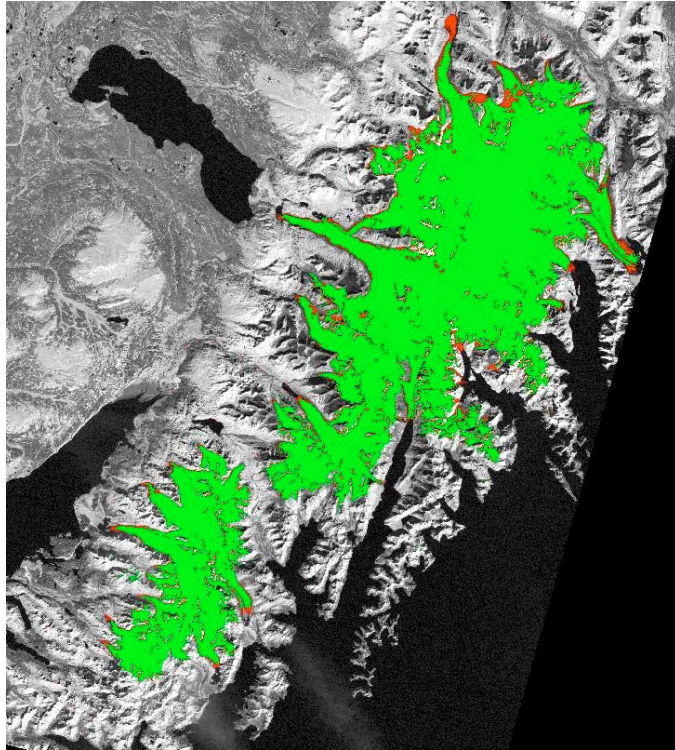


Figure 7. Changes in areal extent from 1986 to 2002. The red represents the area of glacier ice in 1986, and the green represents the area of glacier ice in 2002.

